Powder densification modeling of the Spark Plasma Sintering process

Speaker:
Charles MANIERE[1, 2]

Co-authors:
Claude ESTOURNES[1]
Lise DURAND[2]
Geoffroy CHEVALLIER[1]
Khalid AFANGA[1]
Jean-Baptiste FRUHAUF[3]

[1] CIRIMAT, TOULOUSE , France
[2] CEMES, TOULOUSE, France
[3] SCT, TARBES, France

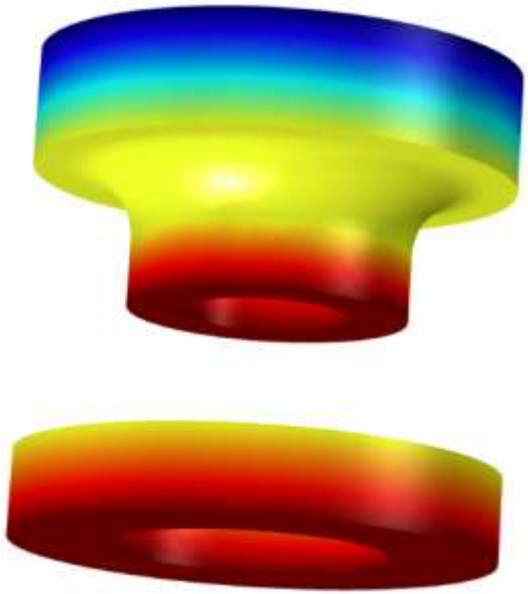

COMSOL CONFERENCE 2014 CAMBRIDGE

Outline

I. Process description

II. General description of implied physics

III. Model implementation

IV. Densification in complex shape

V. Conclusion

I. Process description

> The powder is place between two punches in a die.

> The pulsed current generator create a Joule heating of the powder.

> An external pressure is applied that highly amplify The powder densification kinetics.

> <u>Microstructure control</u> and <u>very low sintering time</u>: few min with SPS, hours with HP

Joule Heating

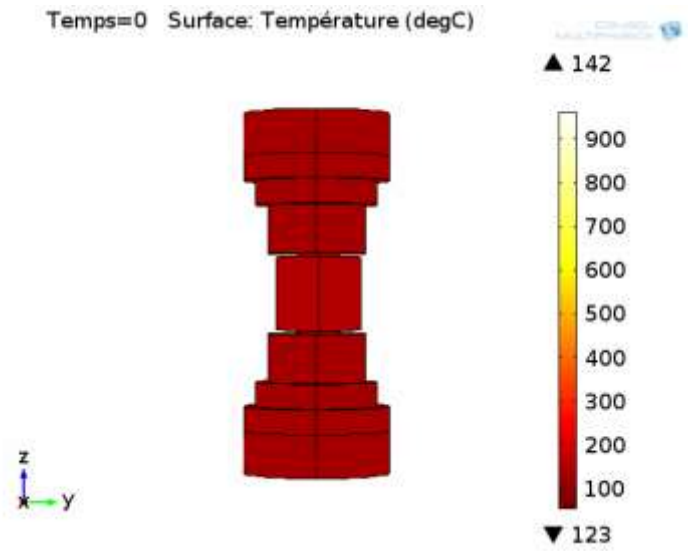

Spark-Plasma-Sintering Process

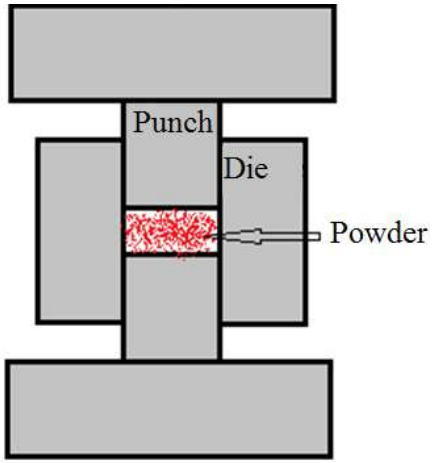

Powder compaction

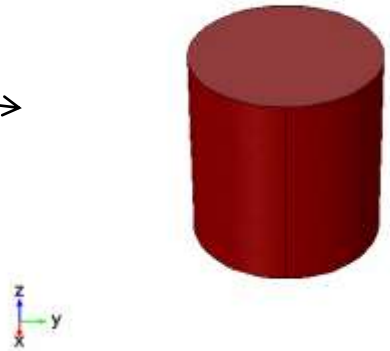

II. General description of implied physics

- Joule heating
- Densification of powder
- Microstructure

Three main physics: Electrical, thermal et Mechanical

Electrical Model:

Current Eq: $\nabla . \vec{J} = 0$

FEM Coupling

Thermal Model:

Heat Eq: $\nabla . (-\lambda \nabla T) + \rho Cp \frac{\partial T}{\partial t} = \vec{J}\vec{E}$

Mechanical Model: Porous creep

	Olevsky Model	Or	Abouaf Model
>Stress tensor:	$\underline{\sigma} = \frac{\sigma_{eq}}{\dot{\varepsilon}_{eq}} \left(\varphi \underline{\dot{\varepsilon}} + \left(\psi - \frac{1}{3}\varphi \right) tr(\underline{\dot{\varepsilon}}) \mathbb{i} \right) + P_l \mathbb{i}$		$\underline{\sigma} = \frac{\sigma_{eq}}{\dot{\varepsilon}_{eq}} \left(\frac{2}{3c} \underline{\dot{\varepsilon}} + \left(\frac{1}{9f} - \frac{2}{9c} \right) tr(\underline{\dot{\varepsilon}}) \mathbb{i} \right)$
> Equivalent creep parameters:	$\dot{\varepsilon}_{eq} = \frac{1}{\sqrt{1-\theta}} \sqrt{\varphi \dot{\gamma}^2 + \psi tr(\underline{\dot{\varepsilon}})^2}$		$\sigma_{eq} = \sqrt{3cJ_2 + fI_1^2}$
> Functions of the porosity:	$\varphi = (1-\theta)^2$ $\psi = \frac{2}{3} \frac{(1-\theta)^3}{\theta}$		$f = k \frac{(1-\rho)}{(\rho - \rho_{cr})}$ $c = 1 + a \frac{(1-\rho)}{(\rho - \rho_{cr})}$

Grain growth law (Olevsky): $\dot{G} = \frac{k_0}{3G^2} \left(\frac{\theta_c}{\theta_c + \theta} \right)^{\frac{3}{2}} exp\left(\frac{-Q_G}{RT} \right)$

III. Model implementation

- The base of the mechanic part of the problem already exist in the structural mechanic module.

$$\nabla \underline{\sigma} = 0$$

- To implement the creep behavior law, we use the Nonlinear materials module.

$$\underline{\sigma} = \frac{\sigma_{eq}}{\dot{\varepsilon}_{eq}}\left(\varphi\,\underline{\dot{\varepsilon}} + \left(\psi - \frac{1}{3}\varphi\right) tr\left(\underline{\dot{\varepsilon}}\right)\mathbb{i}\right) + P_l\mathbb{i}$$

- The mass conservation equation and the grain grow law need to be create.

$$\frac{\dot{\theta}}{1-\theta} = \dot{\varepsilon}_x + \dot{\varepsilon}_y + \dot{\varepsilon}_z$$

- With these last points the base of the powder densification model is implemented. The modeling of the Joule Heating can be easily implemented with the Joule heating module.

Powder compaction

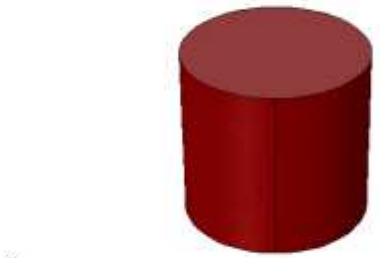

IV. Densification in complex shape

> Problem of thickness differences

> **Simple geometry => uniform densification**

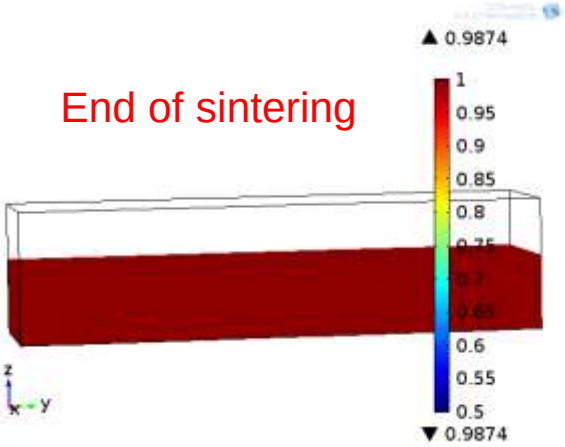

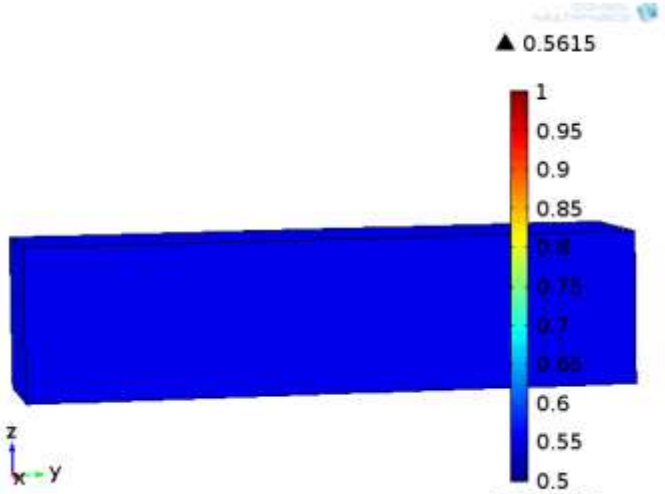

> **Complex shape with thickness difference**
> **=> density differences**

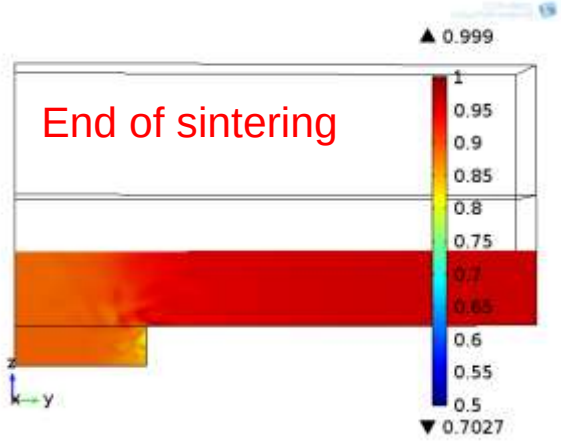

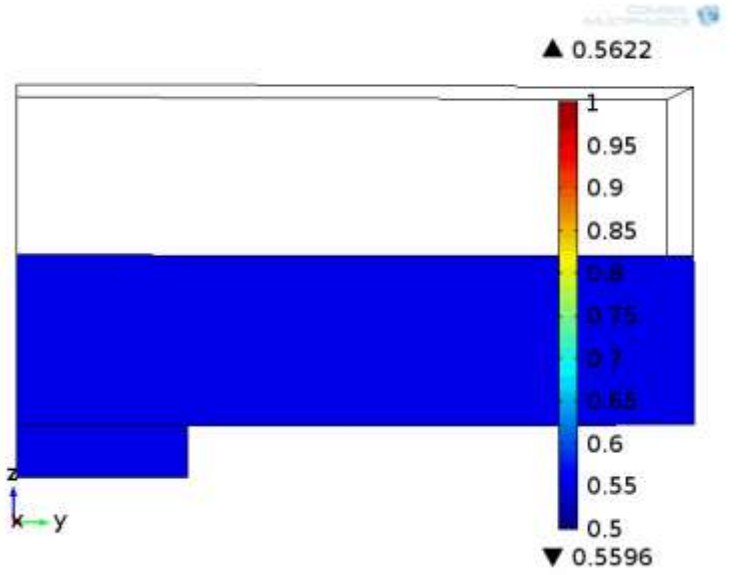

IV. Densification in complex shape

> A practical case

A complex shaped part with a hole and thickness differences

Complex part obtained by free sintering (SCT®)

High thickness differences ⇨ Density differences

Density in final stage of sintering: Complex shaped part

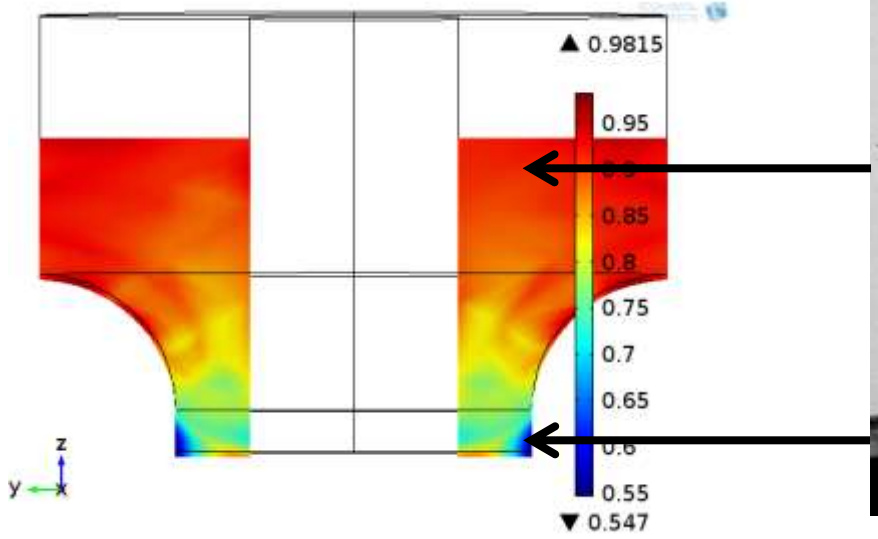

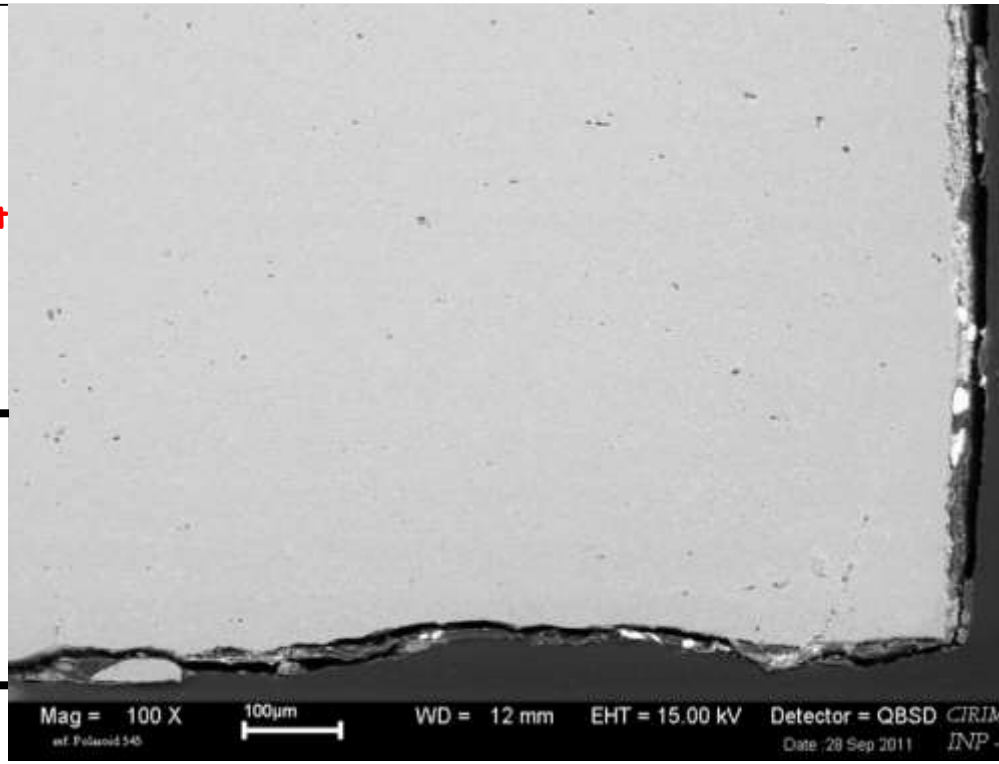

IV. Densification in complex shape

› The use of a sacrificial materials

We introduce a ring of powder to allow the upper part to move down and homogenize the density

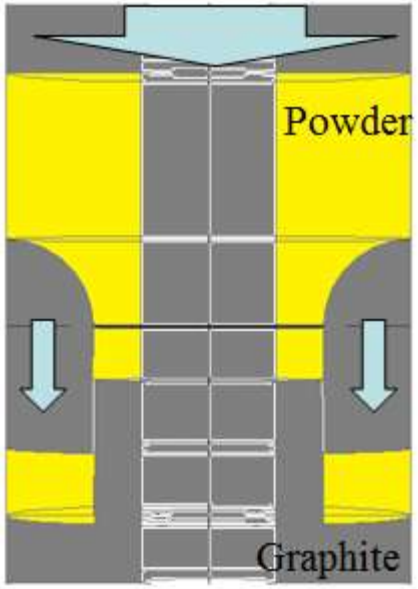

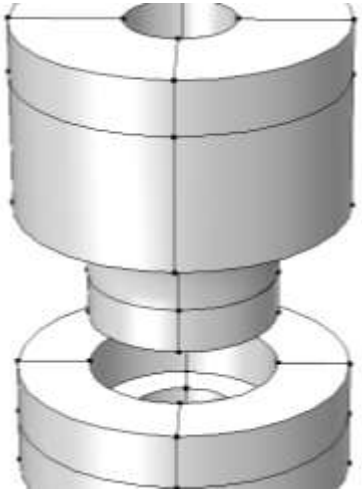

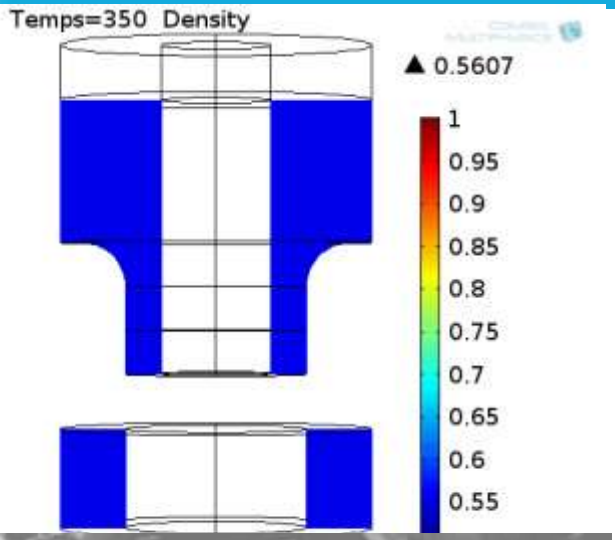

› The complex part is now totally dense

Final density

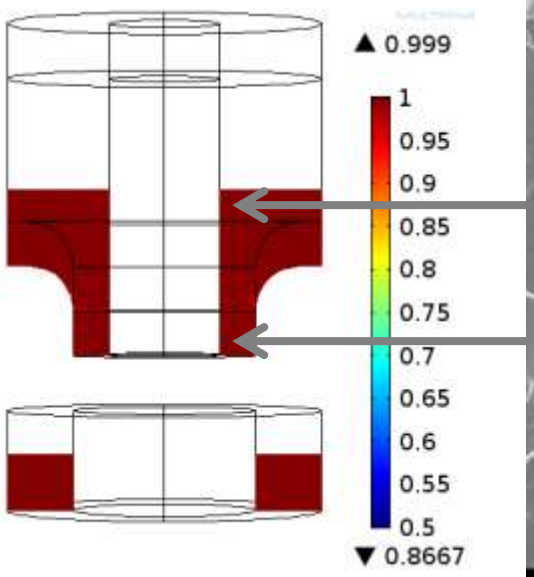

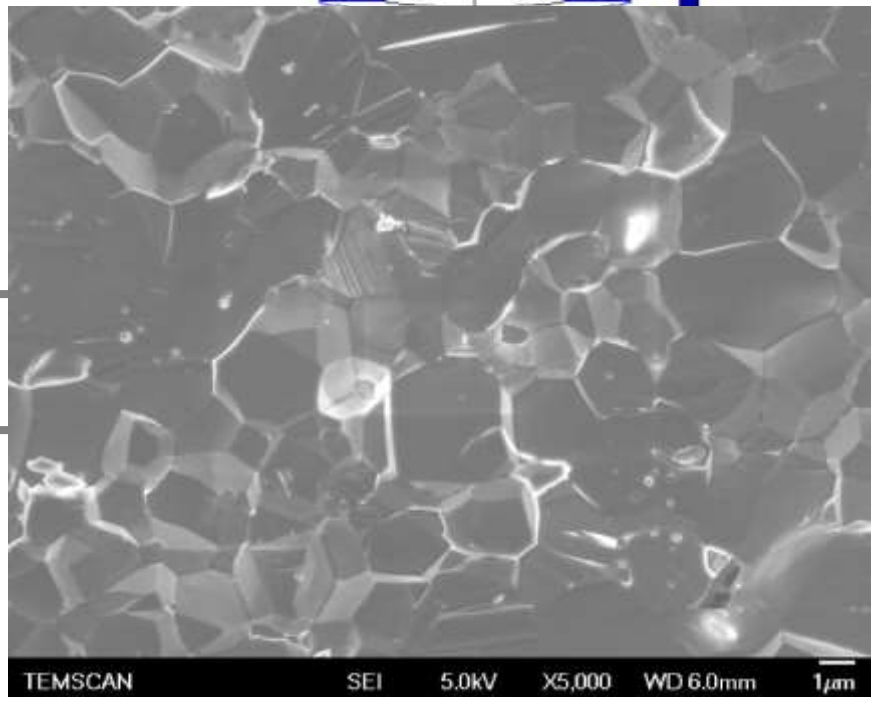

V. Conclusion

- The implementation of the powder sintering without script is possible using the structural and nonlinear module

- This model show that in complex shape a high thickness difference imply at end of cycle high density differences.

- A sacrificial material can be use to correct the thickness difference

INSTITUT CARNOT CIRIMAT

Thank you for your attention

3.2.5.2 Attainment of High Density

As described in Chapter 2, densification occurs by the flux of matter from the grain boundaries (the source) to the pores (the sink). For sintering by diffusion mechanisms, at a given temperature and density, the dependence of the densification rate on the grain size G can be written

$$\frac{1}{\rho}\frac{d\rho}{dt} = \frac{K}{G^m} \tag{3.1}$$

where K is a temperature-dependent constant and the exponent $m = 3$ for lattice diffusion and $m = 4$ for grain boundary diffusion. Rapid densification requires that the diffusion distance between the source of matter and the sink be kept small; that is, the grain size must remain small (Figure 3.5a). According to Equation 3.1, rapid grain growth causes a drastic reduction in the densification rate, so prolonged sintering times are needed to achieve the required density, which increases the tendency for abnormal grain growth to occur. When abnormal grain growth occurs, the pores become trapped inside the grains and become difficult or almost impossible to remove because the transport paths become large, in the case of lattice diffusion, or are eliminated, in the case of grain boundary diffusion (Figure 3.5b). The attainment of high density therefore requires the control of normal grain growth as well as the avoidance of abnormal grain growth.

JOURNAL OF MATERIALS SCIENCE 27 (1992) 2641–2648

Constant heating rate analysis of simultaneous sintering mechanisms in alumina

S. H. HILLMAN*, R. M. GERMAN†
Materials Engineering Department, Rensselaer Polytechnic Institute, Troy, NY 12180-3590, USA

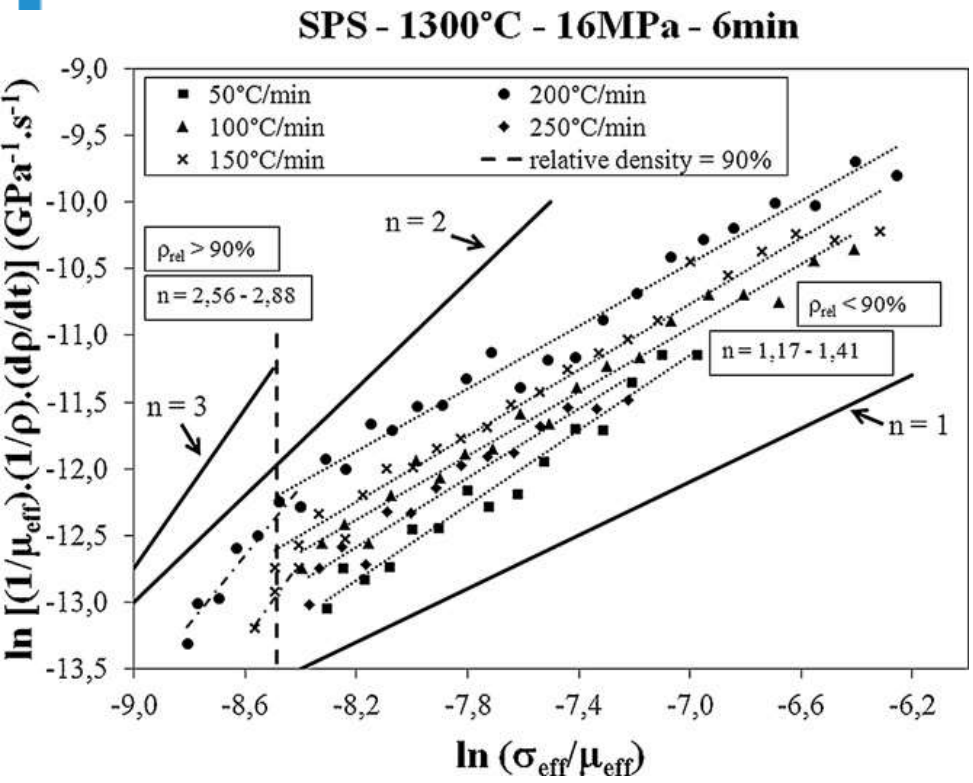

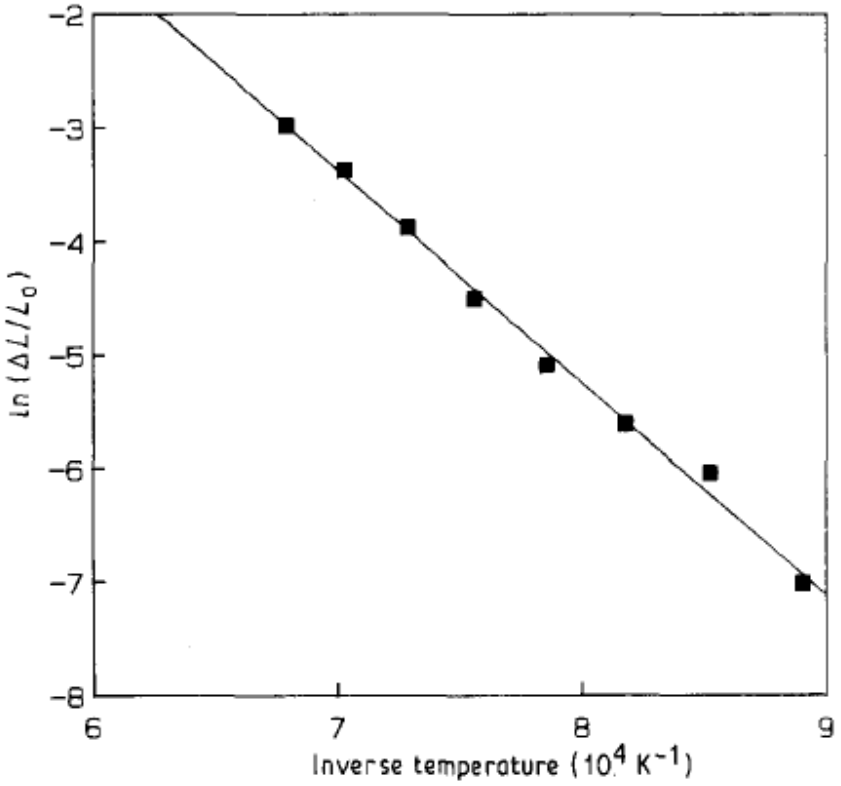

Figure 6 Shrinkage data treated on an Arrhenius plot as the basis for extracting the apparent activation energy at heating rate of 5 K min^{-1}.

TABLE II Surface area reduction and shrinkage activation energy analysis

Mechanism	γ	Q (kJ mol^{-1})	Q/γ (kJ mol^{-1})	Reference
Measured surface area Arrhenius slope, $Q/\gamma = 120$ kJ mol^{-1}				
Volume diffusion	2.7	447	177	35
Grain boundary diffusion	3.3	418	127	36
Surface diffusion	3.6	536	149	37
Measured shrinkage Arrhenius slope, $Q/n = 144$ kJ mol^{-1}				
Volume diffusion	2.5	447	191	35
Grain boundary diffusion	3.0	418	139	36

The temperature dependence of the diffusion coefficient have a Arrhenius form.

$$D = D_0 \exp\left(\frac{-\Delta H_{SD}}{RT}\right) \quad *$$

* E.A.Olevsky, C.Garcia-Cardona, W.L.Bradbury, C.D.Haines, D.G.Martin, D.Kapoor. Fundamental aspects of spark plasma sintering II: Finite element analysis of scalability. Journal of American ceramic society 95 (2012) 2414-2422.

* Responsable du Groupe Thermomécanique-Plasticité, Centre de Mise en Forme des Matériaux, Sophia Antipolis, 06560 Valbonne, GRECO C.N.R.S., Grandes Déformations et Endommagement.

** Directeur, Centre de Mise en Forme des Matériaux, Sophia Antipolis, 06560 Valbonne, GRECO C.N.R.S., Grandes Déformations et Endommagement.

Modélisation numérique de la déformation à chaud de poudres métalliques

A numerical model for hot deformation of metal powders

par

M. ABOUAF* et J. L. CHENOT**

$$\dot{\varepsilon}_{eq} = \rho D^{c}_{eq} = \frac{\partial \Omega}{\partial \sigma_{eq}} = A \sinh (a \sigma_{eq})^{n} \exp(-Q/R\,\theta),$$

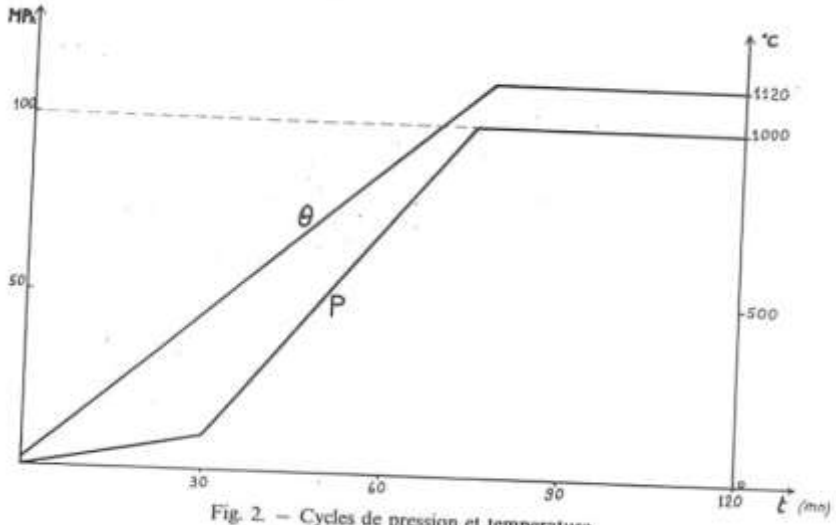

Fig. 2. — Cycles de pression et temperature.

Fig. 2. — Pressure and temperature cycle.

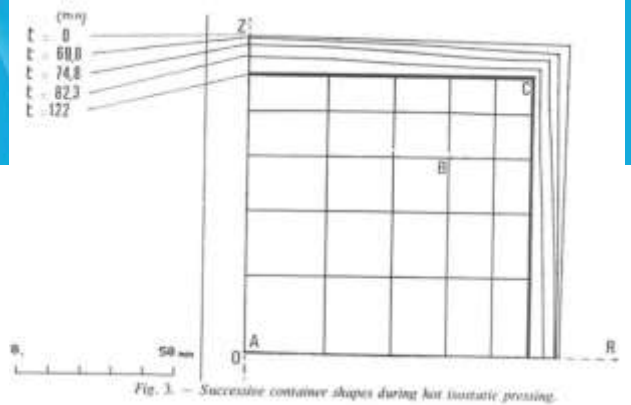

Fig. 3. — *Successive container shapes during hot isostatic pressing.*

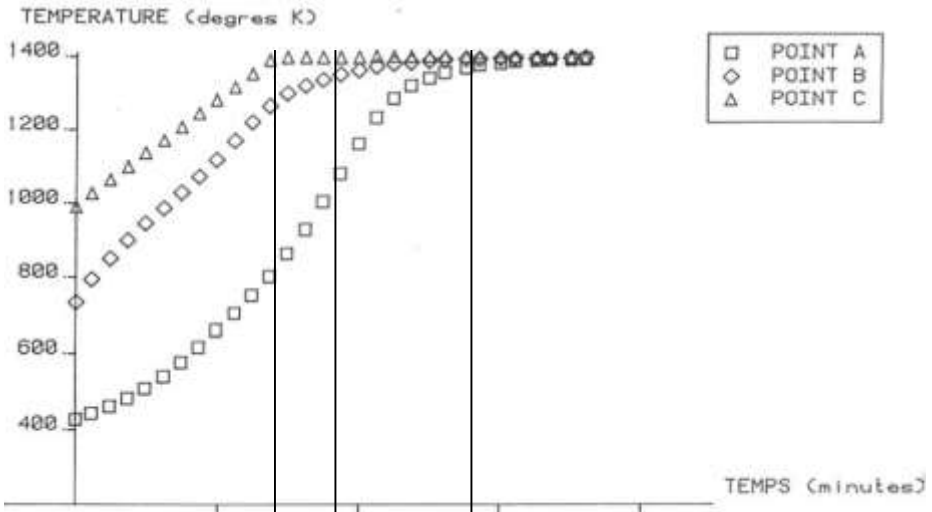

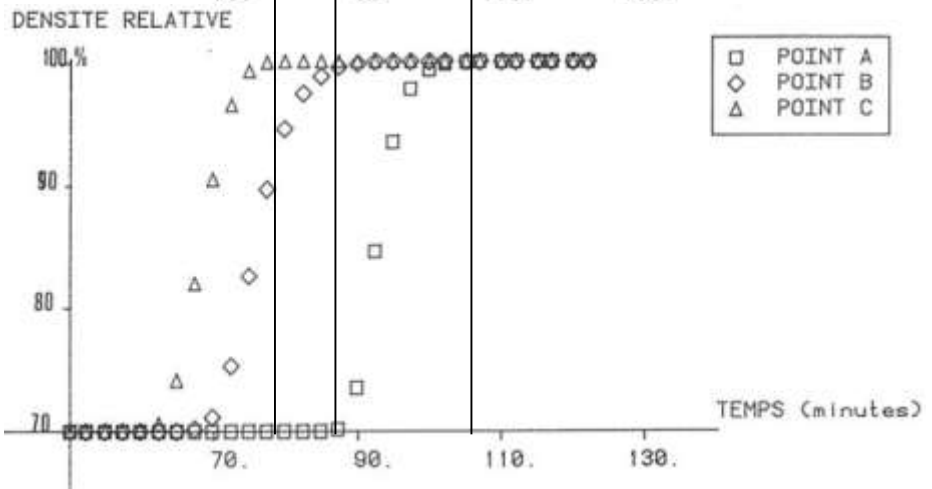

journal

J. Am. Ceram. Soc., 73 [11] 3518–21 (1990)

Deformation and Grain Growth of Low-Temperature-Sintered High-Purity Alumina

Liang A. Xue* and I-Wei Chen*

Department of Materials Science and Engineering, The University of Michigan, Ann Arbor, Michigan 48109–2136

Their deformation can generally be expressed by the following equation:

$$\dot{\varepsilon} = A\sigma^n d^{-p} \exp(-Q/RT) \tag{1}$$

where $\dot{\varepsilon}$ is the strain rate, A is a constant, σ is the flow stress, n is the stress exponent, d is the grain size, p is the inverse grain size exponent, Q is the activation energy, and R and T have their usual meanings. For fine-grained alumina,

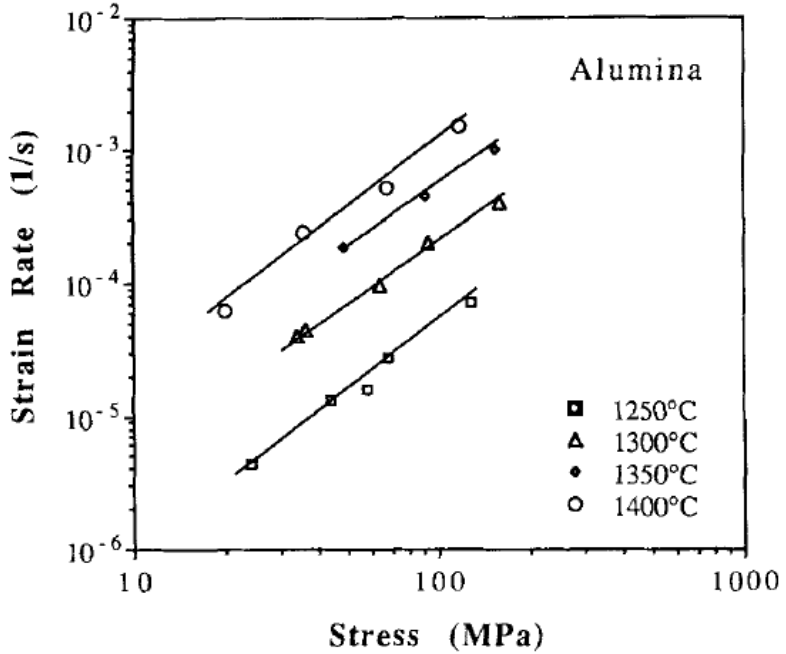

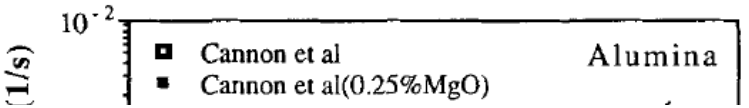

The data of strain rate and flow stress are plotted on a logarithmic scale in Fig. 5(A) at different deformation temperatures. To reduce the influence of grain growth, flow stress at 2% strain was used here. The stress exponent n found from the slopes is about 1.7, which is in reasonably good agreement with the n values of 1.5 to 2 reported for

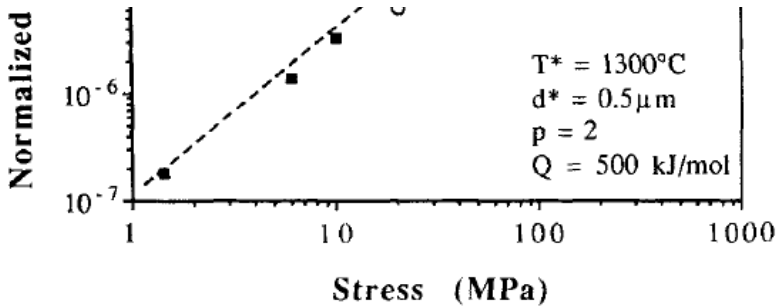

II. The effect of the electric and thermal contact

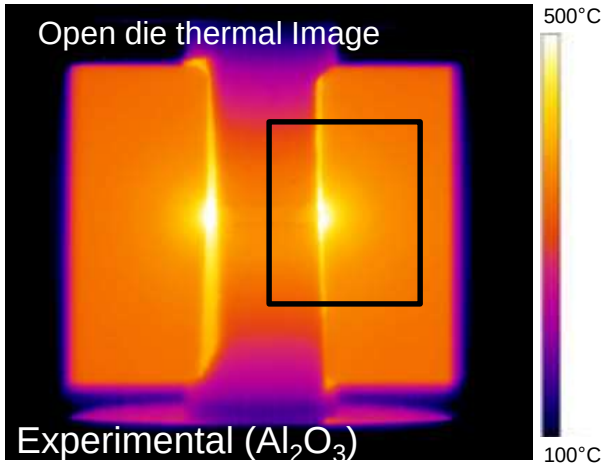

A. Pavia (Phd)

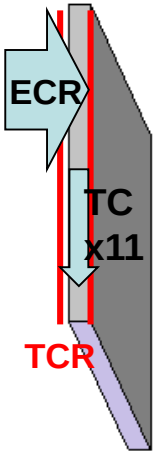

	In plane	through thickness
Electrical resistivity (Ω.Cm) at 20°C	0.001	0.05

- Electric contact is responsible for a global warming of the system

- Thermal contact explains the localized heating of the papyex

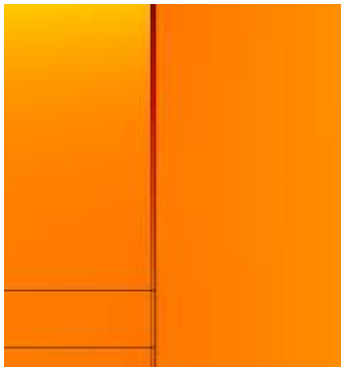

- Correct the thermal conductivity in plane of Papyex creates a hot spot.

- Considering these three parameters it is possible to adjust the modeling temperature with the experiment.